Design and Fabrication Techniques for a Mid-Infrared Photonic Crystal Defect Cavity in Indium Antimonide

J. R. Pugh[1] , Y. L. D. Ho[1], P. J. Heard[1], G. R. Nash[1,2], T. Ashley[2], J. G. Rarity[1] and M. J. Cryan[1]

[1] *University of Bristol, Bristol,BS8 1UB, UK,, jon.pugh@bristol.ac.uk, m.cryan@bristol.ac.uk*

[2] *QinetiQ, Malvern Technology Centre, Malvern, WR14 3PS*

ABSTRACT

Simulation results and fabrication details are presented for a two-dimensional $Al_xGa_yIn_{1-x-y}Sb$ photonic crystal membrane defect cavity. Peak emission is predicted at $\lambda = 3.372$ μm with a *Q* factor of 26233 for an optimized membrane thickness of 1000 nm.

Keywords: Photonic crystal, mid infra-red, focused ion beam, finite-difference time-domain (FDTD).

1. INTRODUCTION

There is a growing demand for semiconductor lasers capable of operating in continuous wave (CW) mode at room temperature in the spectral region from 3 to 4 μm. A wide range of applications include gas detection and remote sensing of pollutants, free space optical communications, health care, manufacturing, security and defence. A detailed survey of progress can be seen in [1]. One possible approach for achieving further reduction in threshold current and increased temperature operation is through the use of photonic crystals (PhC). PhC defect lasers [2] enable one of the smallest possible lasing volumes to be achieved and the very high *Q* factors obtainable [3] will produce very low threshold current devices which could improve their temperature performance. This paper presents the design, fabrication and initial measuring of a prototype device based on Focused Ion Beam (FIB) etching in the fore-mentioned AlGaInSb system [4]. There are damage issues associated with FIB processing but annealing and careful choice of FIB etching procedure can minimize these [5]. The 3D Finite Difference Time Domain (FDTD) method has been used to design the initial prototype [6-8].

2. PHOTONIC BAND GAP DEFECT LASERS AND DEVICE DESIGN

Light can be localized in all three dimensions using the combination of a 2D photonic crystal [9] and a membrane with a lower refractive index medium, such as air, above and below [10]. To create a PhC defect laser, a 2D pattern of holes is designed to forbid the transmission of light at the desired wavelength. A defect is then introduced into the array of holes which will act to confine light if the wavelength is within the band gap. The defect can have any shape or size; it can be made by changing the refractive index of a hole (filling with another material), modifying its radius, or removing it altogether. The photonic crystal pattern including the defect, is then etched into the membrane which in our case is an $Al_xGa_yIn_{1-x-y}Sb$ material system where gain is provided by two strained quantum wells (*Q*Ws) separated by barriers [4]. The governing properties of the photonic crystal are the 2D hexagonal geometry, the refractive index of the host material, the lattice constant, *a*, and the radius of the air holes, *r* [9]. This study is restricted to TE modes (E-field perpendicular to hole axis) since this is the dominant polarization emitted by the *Q*Ws and there is no overlap of the TM induced Γ-M and Γ-K photonic bandgaps. These were calculated using two online available software packages, a one-dimensional mode solver (OMS) [11] to find the effective index, n_{eff}, and a 2D model which uses the Translight implementation of the transfer matrix method [12]. Most PhC defect lasers tend to use membrane structures with air above and below [10]. This gives very good vertical confinement of light and leads to very high *Q* factor cavities. Typically these membranes are around $0.6a$ thick in order to maximize the photonic band gap [13]. However, as stated in [13], maximizing the band gap may not result in optimum performance for a given parameter. In the case of *Q* factor a number of studies have shown that thicker membranes can lead to stronger confinement [14].

Whilst the effect of slab thickness has been studied for single defect cases, less work has been done for L3 defects and modified L3 defects that can result in very high *Q* factors due to gentle confinement of the mode [3]. This paper will study this case and shows that dramatic increases in *Q* factor can occur when the optimum slab thickness coincides with the optimum in-plane confinement geometry. The maximum membrane thickness that allows only the propagation of the fundamental mode of wavelength 3.4 μm is ~460 nm, calculated using a simple average refractive index of the membrane structure, n_{av}. Therefore, the initial membrane thickness chosen is 400 nm, with two thicker membranes at 800 nm and 1000 nm also considered.

3. 3D FDTD ANALYSIS OF DEFECT MODES

An in-house FDTD has been used and the simulation space is meshed in all three dimensions by a uniform 50 nm grid and truncated on all but one sides by Mur absorbing boundaries. *x* is perpendicular to the defect but in the membrane plane, *y* is perpendicular to the membrane plane, and *z* is parallel with the line of the L3 defect.

The simulation is symmetrical in x so the addition of an electric wall at the centre point of the structure on the x-axis allows us to reduce the simulation size by half, resulting in a simulation consisting of 4.3 million cells requiring 427 MB of RAM over a 21 hour runtime for 100,000 iterations on a Pentium 4 processor. Further symmetry reduction is possible and will be addressed in future work. The mesh has a resolution of greater than 17 cells per wavelength for frequencies within the photonic bandgap which guarantees good accuracy for the method. A Gaussian modulated sinusoid source, of width 1 cell, is centrally located within the defect and polarized in the x-direction in order to excite the TE-like modes. A probe, measuring the six field components with respect to time is placed one cell away from the defect centre. Frequency snapshots are placed at the peak wavelengths of cavity resonances and are located at the centre of the membrane in the y-plane, one cell away from the x-symmetry plane, and as a line through the centre of both the defect and membrane. A frequency snapshot is created by performing a running Fourier transform at a user defined wavelength at each mesh point in a plane. To calculate the Q-factor of the resonant modes, an online available program 'Harminv', developed by MIT, is used [13]. This reduces the number of time steps required in the simulation by around a factor 10 to get the same value of Q compared to a more conventional approach. In each case, two distinct resonance peaks are detected, one at ~3.4 μm and one at ~3.9 μm, referred to as mode 1 and mode 2 respectively in this paper.

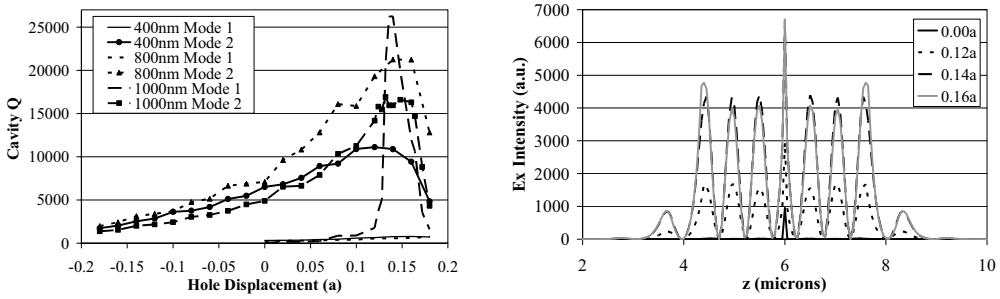

(a) (b)

Fig. 1: (a) The effect of displacing the hole either side of the cavity along z for the 400 nm, 800 nm and 1000 nm thick membranes. Positive values of displacement mean the hole is moving away from the defect centre, (b) E_x intensity with respect to z for mode 1 with hole displacements of 0.00a (resonance at 3.317 μm), 0.12a (3.331 μm), 0.14a (3.375 μm) and 0.16a (3.384 μm) for a 1000 nm thick membrane.

As shown in Fig. 1(a), mode 2 sees a large increase in Q in the 400 nm and 800 nm membranes with increasing hole displacement until it drops at displacements larger than ~0.16a, and mode 1 also sees an increase although far smaller in comparison. Finally, a very different behavior is observed in the 1000nm cavity results. Two modes occur as in the case of the other membrane thicknesses and mode 2 increases in Q in a similar way. However, here mode 1 dramatically increases its Q factor at an offset of 0.14a. These very surprising results cannot simply be explained by gentle confinement alone, since it is very different in the case of thinner membranes. Similar studies in H1 cavities [14] have observed this effect and a clear understanding in this case has been obtained. These results are the first time such effects have been observed in L3 modified cavities which can have much higher Q factors than H1 cavities and thus the potential for very high Q factors is opened up. The origin of the rapid increase in Q factor comes from a second effect combined with gentle confinement: vertical cavity resonance. It is well known that slabs with thicknesses of multiples of the guided wavelength, $(\lambda_g = \lambda_o / n_{eff})$, will give enhanced vertical confinement. Here, for mode 1 in the 1000 nm membrane we have $\lambda_g = 3.372\ \mu m / 3.596 = 0.9385\ \mu m$ and thus $d/\lambda_g = 1.0656$. Whereas for the 800 nm case resonating at 3.9139 μm, we have $\lambda_g = 3.9139\ \mu m / 3.4320 = 1.1404\ \mu m$ and thus $d/\lambda_g = 0.7015$. This results in the slowly increasing Q factor in the 800 nm case, since it is far from $d/\lambda_g = 1$. In the case of mode 2 in the 1000 nm membrane we have $\lambda_g = 3.900\ \mu m / 3.5430 = 1.1008\ \mu m$ and thus $d/\lambda_g = 0.9085$, which is similar to the case for the mode 1, so the question arises as to why mode 1 sees such a dramatic increase, and not mode 2. It is believed this is due the fact that mode 2 has better Gaussian distribution. A further question arises as to why the maximum Q factor occurs at a hole displacement of 0.14a. This can be understood by looking the E_x field line cuts through the centre of the cavity which are shown in Fig. 1(b) for 3 different displacements and no displacement which is at a very low intensity. It can be seen for a displacement of 0.14a a slightly more Gaussian shape is obtained which appears to result in a very sharp increase in Q factor. In future work full 3D dispersion diagrams will be used to further the understanding of the interesting effects observed here and further FDTD modelling will be used to optimize the cavity Q.

4. DEVICE PROTOTYPE FABRICATION

Previously, photonic crystal defect cavities have been FIB etched into vertically oriented membranes containing QWs [6], we believe this to be the first example of FIB etching of an "in-plane" membrane containing QWs. A multi-step FIB fabrication procedure was then developed to perform all other etches without removal of the

device from the chamber; this required the device to be mounted on an angled stub. The 30° angle of the stub, along with the 60° rotational freedom of the FIB workstation stage, allows multiple etches to be carried out on one device at angles normal to each other. An initial coarse etch was performed at a beam current of 1000 pA, with a beam diameter of 20 nm and accelerating voltage of 30 keV which is constant for all etches. To achieve a smooth facet, making fine detail such as the *Q*Ws visible, an etch was performed at a beam current of 150 pA. To compensate for any lateral etching, angular tilt was set to 1.5° for all etches. A stream file in the FEI Strata FIB201 has a maximum size of 10^6 points, so the PhC can be split into several sections allowing etching to be carried out at higher magnification resulting in better resolution of the stream file. This also helps to keep the etching time down minimizing any effect of beam-drift on the pattern. PhC holes with near vertical sidewalls are produced for a 1 µm membrane using a raster-scan stream file with a dwell time of 800 µs with 25 repetitions at a beam current of 11 pA. An example prototype of a 1µm membrane is shown in Fig. 2.

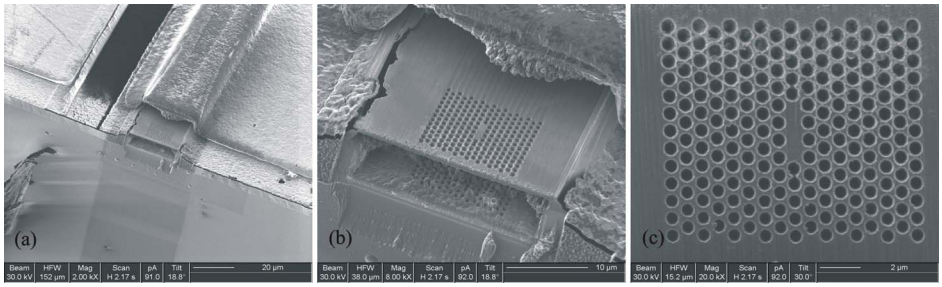

Fig. 2. Images of the 1µm thick PhC membrane taken by the FIB, (a) a view of the top-side of the membrane after etching away the bulk material and the PhC holes, (b) a closer view of (a) and (c) a plan view of the PhC structure etched through the membrane.

Hopman *et al.* [15] showed that spiral milling can also be utilized by the fib to achieve holes with a more circular profile and straighter sidewalls. This technique is also advantageous as there will be a single pass of the beam between each hole as opposed to the raster technique, where multiple passes of the beam between holes induces membrane surface damage. Figure 3 shows images of four holes etched through the 1 µm thick membrane with a 4 pA beam current and a stream file with 5, 10, 15 and 20 repetitions and a dwell time of 10 ms.

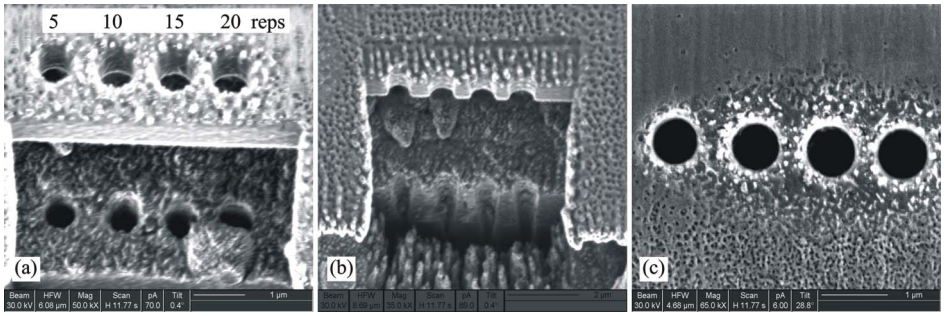

Fig. 3. Images of 4 holes with pattern repetitions of 5, 10, 15 and 20 etched through a 1µm thick PhC membrane taken by the FIB, (a) an angled view of the top-side of the membrane and the bottom side of the undercut, (b) a cross-sectional view of (a) and (c) a plan view of the holes etched through the membrane.

The large degree of surface damage is due to repeated imaging of the sample to demonstrate the hole shape. Very straight sidewalls of ~1º are shown. The designed diameter of the holes is 618.8 nm and the actual diameter is 660 nm, 680 nm, 700 nm and 720 nm for 5, 10, 15 and 20 repetitions, respectively. Over-milling when using spiral milling is consistent with Hopman *et al.* and will need to be accounted for in future stream file design.

5. DEVICE MEASUREMENTS

Initial device measurements have been carried out on a sample before and after the first stage of FIB fabrication – forming the 1 µm thick membrane. The emittance is plotted with respect to applied current for varying temperature for the un-etched and FIB etched devices. Figure 4 shows the plots for the two cases, with a resulting order of magnitude decrease in the emittance from the FIB etched device as compared to the unetched device. However, after FIB etching the device, it still behaves in a similar way, showing that this stage of the FIB etching procedure is possible without causing catastrophic damage to the device. The same procedure will now be followed with regard to etching the holes through the membrane.

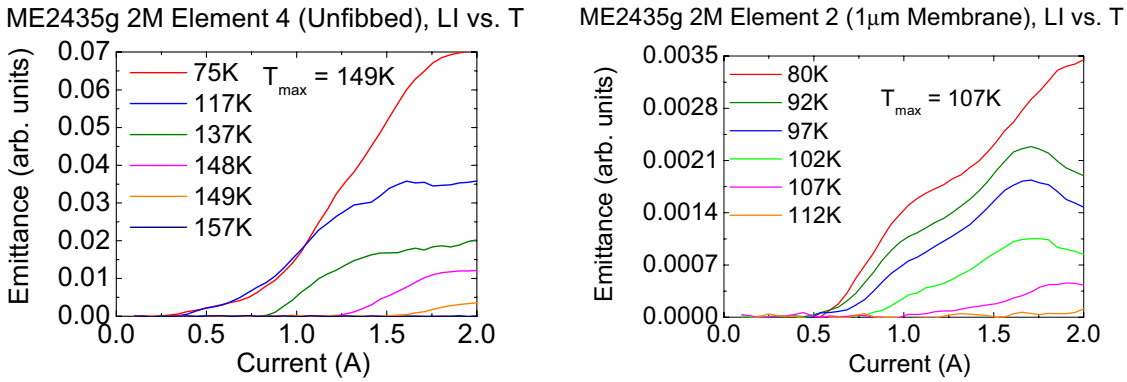

Fig. 4. Emittance (a.u.) vs. current (A) curves for varying operating temperature for (a) an un-etched device and (b) a FIB etched 1μm membrane.

6. CONCLUSION

This paper presents the design and fabrication of a membrane based PhC defect cavity in the AlGaInSb material system for use in the 3-4μm wavelength range. The design is based on a modified L3 cavity using gentle confinement to enhance the cavity *Q*. A study has been carried out on the effect of different membrane thickness and it is shown that vertical cavity resonance combined with gentle in-plane confinement can result in very dramatic increases in cavity *Q*. FIB etching is then used to create a membrane at the facet of a conventional Fabry-Perot laser and etch the PhC design into the membrane. The 1 μm thick membrane device has been fabricated and assessed using photoluminescence testing showing a decrease in emittance but no change in behaviour. The FIB etch process can induce damage, especially to sensitive structures such as *Q*Ws, but careful annealing and use of metal masking techniques can significantly reduce these problems. This study is a precursor to a wafer scale electron beam fabrication process and having performed this FIB based study will dramatically reduce the costs and time associated with this process.

REFERENCES

[1] J.R. Pugh *et al.*, "Design and fabrication of a midinfrared PhC defect cavity in indium antimonide", *J. Opt. A: Pure Appl. Opt* **11** (2009).
[2] O. Painter *et al.*, "Two-Dimensional Photonic Band-Gap Defect Mode Laser", *Science* **284** 1819-1821 (1999).
[3] Y Akahane *et al.*, "Fine-tuned high-*Q* photonic-crystal nanocavity" *Optics Express* **13** 4 (2005).
[4] G.R. Nash *et al.*, "Midinfrared GaInSb/AlGaInSb quantum well laser diodes grown on GaAs", *App. Phys. Lett.* **91** 131118 (2007).
[5] M.J. Cryan *et al.*, "FIB-based fabrication of nanostructured photonic devices", *IEEE J. of Sel. Top. in Quant. Elec.* **11** 6 1266-1277 (2005).
[6] M. Lončar *et al.*, "Design and fabrication of photonic crystal quantum cascade lasers for optofluidics" *Optics Express* **15** 8 (2007).
[7] Y.L.D. Ho *et al.*, "Three-dimensional FDTD simulation of micro-pillar microcavity geometries suitable for efficient single-photon sources", *IEEE Journal of Quantum Electronics* **43** 6, 462-472 (2007).
[8] K.S. Yee *et a.l*, "Numerical solution of initial boundary value problem involving Maxwell's equations in isotropic media", *IEEE Trans. Antennas Propagat.* **AP-14**, 302-306 (1966).
[9] E. Yablonovich *et al.*, "Inhibited Spontaneous Emission in Solid-State Physics and Electronics", *Phys. Rev. Lett.* **58** 20 (1987).
[10] O. Painter *et al.*, "Defect modes of a two-dimensional photonic crystal in an optically thin dielectric slab", *J. Opt. Soc. Am. B* **16** 2 (1999).
[11] M. Hammer, "*OMS, 1-D multilayer slab waveguide mode solver*", [Computer Software] University of Twente, The Netherlands (2008).
[12] A.L. Reynolds, "*Translight*" [Computer Software] Photonic Band Gap Materials Group, University of Glasgow, Scotland (2000).
[13] S.G. Johnson *et al.*, "Guided modes in photonic crystal slabs", *Phys. Rev. B* **60** 8 (1999).
[14] A. Tandaechanurat *et al.*, "Design of photonic crystal microcavities in diamond films", *Optics Express* **16** 1 (2008).
[15] W.C.L. Hopman *et al.*, "Realization of 2-dimensional air-bridge silicon photonic crystals by focused ion beam, milling and nanopolishing", *Proc. SPIE* **6182** pp. 167-173, (2006).